

An Ordered and Fail-Safe Electrical Network in Cable Bacteria

Raghavendran Thiruvallur Eachambadi, Robin Bonné, Rob Cornelissen, Silvia Hidalgo-Martinez, Jaco Vangronsveld, Filip J. R. Meysman, Roland Valcke, Bart Cleuren, and Jean V. Manca*

Cable bacteria are an emerging class of electroactive organisms that sustain unprecedented long-range electron transport across centimeter-scale distances. The local pathways of the electrical currents in these filamentous microorganisms remain unresolved. Here, the electrical circuitry in a single cable bacterium is visualized with nanoscopic resolution using conductive atomic force microscopy. Combined with perturbation experiments, it is demonstrated that electrical currents are conveyed through a parallel network of conductive fibers embedded in the cell envelope, which are electrically interconnected between adjacent cells. This structural organization provides a fail-safe electrical network for long-distance electron transport in these filamentous microorganisms. The observed electrical circuit architecture is unique in biology and can inspire future technological applications in bioelectronics.

Cable bacteria are filamentous microorganisms consisting of more than 10^4 cells, forming unbranched filaments of up to several centimeters long.^[1,2] These bacteria thrive in both freshwater^[3,4] and marine sediments,^[5–7] and couple the oxidation of sulfide within deeper strata of the sediment to the reduction of oxygen near the sediment–water interface. The spatial

segregation of these redox half-reactions across centimeter distances necessitates electron transport, which occurs internally along the length of the filament.^[8–10] While nanometer-scale electron transport is known to occur in prokaryotes, chloroplasts, and mitochondria,^[11–14] and micrometer-scale electrical currents are measured in the nanowire appendages of bacteria and archaea,^[15–19] the centimeter-scale electron transport by cable bacteria extends the known length scale of biological transport by several orders of magnitude.^[2]


While some aspects of the physiology and overall metabolism of cable bacteria have been recently resolved,^[20,21] the mechanism of long-distance electron transport (LDET) inside cable bacteria

remains elusive. Scanning electron microscopy (SEM) and atomic force microscopy (AFM) have shown that the surface of cable bacteria has a unique topography, with parallel ridges running along the entire length of the filaments.^[8,22,23] At the junction between two cells, a “cartwheel” structure (**Figure 1A**) is observed,^[22] of which the composition and function is still

R. Thiruvallur Eachambadi, R. Bonné, Dr. R. Cornelissen, Prof. J. V. Manca
UHasselt – X-LAB
Faculty of Sciences
Hasselt University
Agoralaan – Building D, Diepenbeek B-3590, Belgium
E-mail: jean.manca@uhasselt.be

S. Hidalgo-Martinez, Prof. F. J. R. Meysman
Department of Biology
University of Antwerp
Universiteitsplein 1, Wilrijk B-2610, Belgium

Prof. J. Vangronsveld
Centre for Environmental Sciences
Hasselt University
Agoralaan – Building D, Diepenbeek B-3590, Belgium

 The ORCID identification number(s) for the author(s) of this article can be found under <https://doi.org/10.1002/adbi.202000006>.

© 2020 The Authors. Published by WILEY-VCH Verlag GmbH & Co. KGaA, Weinheim. This is an open access article under the terms of the Creative Commons Attribution-NonCommercial-NoDerivs License, which permits use and distribution in any medium, provided the original work is properly cited, the use is non-commercial and no modifications or adaptations are made.

Prof. J. Vangronsveld
Department of Plant Physiology
Faculty of Biology and Biotechnology
Maria Curie-Skłodowska University
Lublin 20-033, Poland

Prof. F. J. R. Meysman
Department of Biotechnology
Delft University of Technology
Van der Maasweg 9, Delft 2629 HZ, The Netherlands

Prof. R. Valcke
UHasselt – Molecular and Physical Plant Physiology
Faculty of Sciences

Agoralaan – Building D
Hasselt University
Diepenbeek B-3590, Belgium

Prof. B. Cleuren
UHasselt – Theory Lab
Faculty of Sciences
Agoralaan – Building D, Diepenbeek B-3590, Belgium

DOI: 10.1002/adbi.202000006

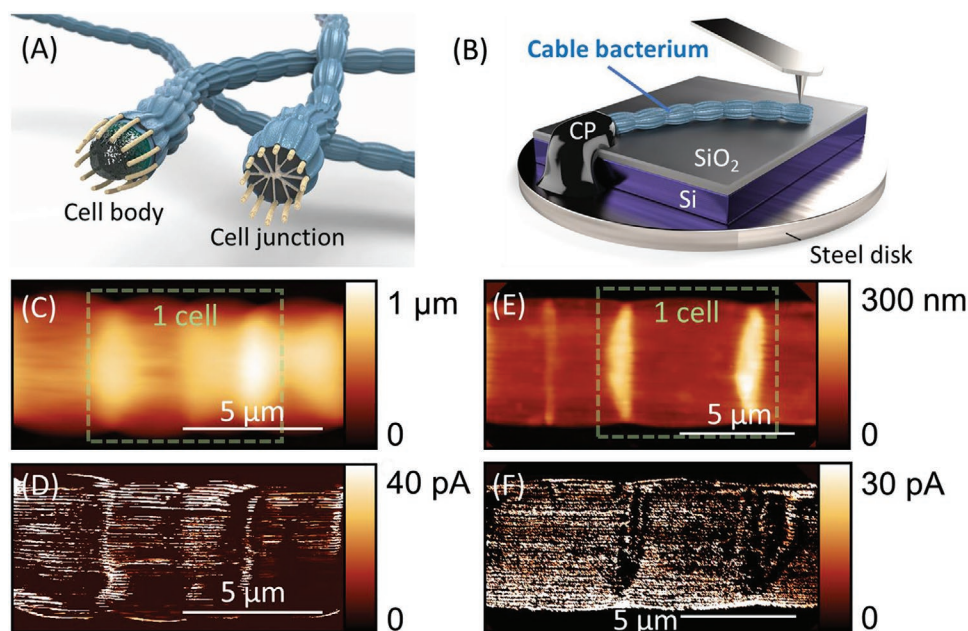


Figure 1. Conductive AFM measurements were performed on cable bacterium filaments for nanoscale topography and electrical current mapping. A) Geometric model: a cable bacterium is a filament of thousands of cells containing fibers that run continuously in the periplasmic space along the filament.^[22] In the junction between two cells, a “cartwheel” structure is present, for which the function and composition is unknown. B) C-AFM measurement set-up: a single cable bacterium filament is placed on a silicon (Si) substrate with silicon oxide (SiO₂) top layer for electric response imaging. The C-AFM functions as a two-electrode system, with one end of the bacterium connected via carbon paste (indicated by CP) to a steel disk, while the other end is probed with the AFM tip with a potential applied between the two electrodes. C–F) C-AFM imaging shows that electrical currents are flowing through parallel pathways in both C,D) intact filaments and E,F) fiber sheaths of cable bacteria. Panels (C) and (E) represent height images, panels (D) and (F) represent current images.

unknown. Initial electrostatic force microscopy (EFM) experiments have shown a distinct elevation of electrostatic forces over these ridges, suggesting the presence of underlying polarizable structures that possess a charge storage capacity.^[8] Subsequent electron microscopy imaging has revealed a parallel network of fibers embedded within the periplasm underneath the ridges. This periplasmic fiber network can be selectively extracted from the cell envelope of the cable bacteria,^[22] thus retaining a so-called fiber sheath, and electrical probe measurements have demonstrated that this fiber sheath harbors conductive material enabling long-range electron transport in cable bacteria.^[24] The parallel fibers make up the majority of the biomass material in the fiber sheath, and so the hypothesis was coined that the periplasmic fibers could be the conductive pathways within cable bacteria.^[24] However, as the fiber sheath retains more periplasmic material than the fibers alone, the conductance of individual fibers was not certified.

In order to precisely pinpoint the location and organization of the conductive pathways within cable bacteria, we employed conductive atomic force microscopy (C-AFM). This technique enables to measure simultaneously the topography of a material together with the electric current flow at the contact point with the surface, and has been previously used to demonstrate conductance of the surface appendages of metal-reducing bacteria^[15,25] and cyanobacteria.^[26] In addition, we designed dedicated perturbation experiments, where we deliberately interrupted the conductive pathways in order to investigate the electrical robustness of damaged cable bacteria with respect to LDET.

In a first experiment, an intact filament was isolated from a sediment enrichment culture and placed on a nonconductive SiO₂ substrate in the C-AFM setup under N₂ atmosphere (see the Experimental Section). At one end of the filament, an electrical connection was established with conductive carbon paste, whereas the other end was left free for electrical current imaging with the C-AFM probe (Figure 1B). The C-AFM setup thereby functions as a two-electrode system: when a voltage is applied between the (movable) probe and the (fixed) electrical contact, the detection of a current indicates the presence of a conductive pathway within the cable bacterium filament. The stability of filament conductance under the N₂ atmosphere was verified (see the Supporting Information).

Initial C-AFM measurements on intact filaments were performed using soft SCM-PIT-V2 probes (see the Experimental Section). A first scan of the surface revealed almost no electrical response signal, indicating that the conductive pathways cannot be directly contacted at the surface of the cable bacterium filament (Figure S1A,B, Supporting Information). After consecutive scanning of the same area, a few conductive spots appeared (Figure S1C,D, Supporting Information), suggesting that conductive structures were embedded underneath the surface, covered by an insulating layer.

When we adapted our scanning procedure and used a stiff diamond coated CDT-NCLR probe (specified in the Experimental Section), a clear electrical response pattern became apparent from the very first scan (Figure 1C,D). Parallel conducting lines were observed along the length of the filament, spatially separated from each other by nonconductive zones

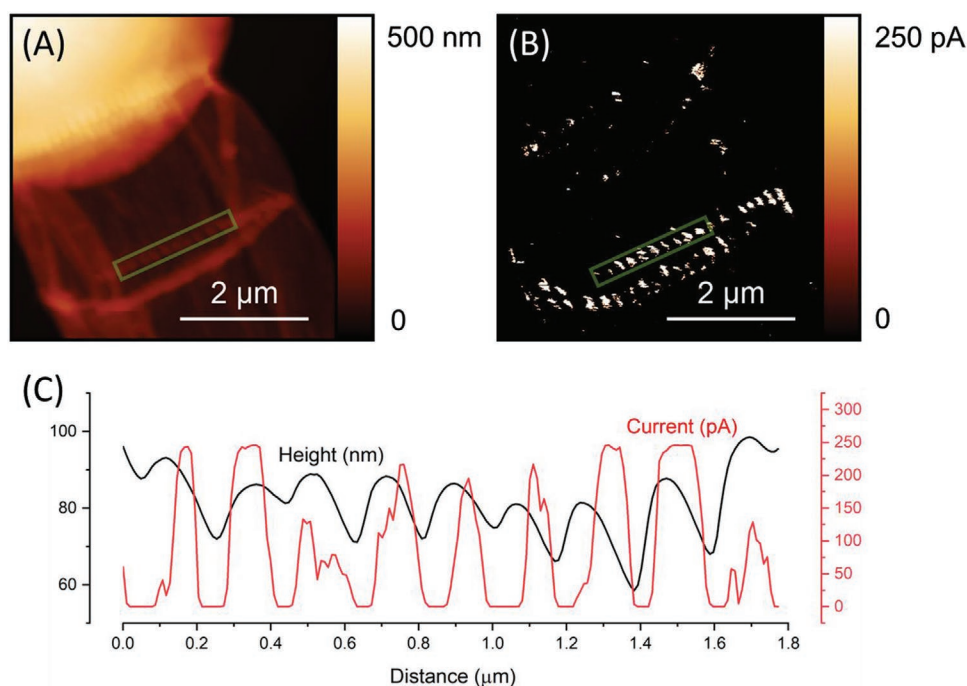


Figure 2. C-AFM imaging of a cable bacterium fiber sheath demonstrates that periplasmic fibers are the conductive structures. A) Height and B) current profiles of the fiber sheath. C) A transect line profile obtained within the green rectangle indicated in panels (A) and (B). The location of the fibers (maxima in the height profile; black curve) corresponds to locations with zones of increased current flow (red curve).

($n = 8$ filaments examined; $m = 37$ areas in total scanned, see statistical analysis). Note that the nonconductive surface layer is not equally well removed at all places, and so only some areas appear conductive. After only two scans, the current signal within a given area typically vanished again. This suggests that the stiff AFM tip scrapes off the insulating outer layer at the first scan, and keeps on removing material in subsequent scans, leading to the conductive fibers being scraped away. This gradual removal of material was confirmed in consecutive images: after about ten consecutive scans the entire cable bacterium filament was sheared off and abraded material was deposited outside the imaged area (Figure S2, Supporting Information). A coarse calibration of the AFM height data (Ten abrasive scans remove ≈ 500 nm height of cable bacterium material) indicates that the conductive fiber structures must be contained within a <100 nm narrow zone, which agrees well with previous fiber thickness characterizations (≈ 50 nm).^[22]

To demonstrate that the periodicity of the observed conductive pattern coincides with the previously reported fiber network in the cell envelope of the cable bacteria, we subjected filaments to a SDS/EDTA extraction procedure that removes the cytoplasm and membranes.^[22] This extraction leaves behind a so-called fiber sheath, which embeds the regularly spaced periplasmic fibers (diameter ≈ 50 nm, with an interspacing of ≈ 200 nm) in a rigid basal sheath.^[22] Recently, macroscopic electrical measurements have shown that this fiber sheath endows the conductivity upon cable bacterium filaments,^[24] but no direct proof was obtained that the fibers are truly guiding the electrical currents. As was done for intact filaments above (Figure 1C,D), we performed C-AFM imaging of fibers sheaths with stiff diamond coated CDT-NCLR probes

(Figure S3, Supporting Information) and stiff PPP-NCLPt probes (Figure 1E,F), which also revealed the ordered pattern of conductive parallel pathways.

To correlate electrical current signals with height measurements, we performed scans on fiber sheaths with a SCM-PIT-V2 probe (Figure 2A,B). In a transect perpendicular to the fiber direction, conductive zones were separated by nonconductive interspacing (Figure 2C). The zones where a current was measured corresponded to the elevated regions caused by the fibers (Figure 2C), and a peak-to-peak width for the current profile (194 ± 20 nm) matched that in the height profile (191 ± 19 nm). These values are also congruent with the fiber interspacing as previously reported.^[22] Overall, these results unequivocally demonstrate that the periplasmic fibers are the conductive structures in cable bacteria.

Cable bacteria hence contain a set of parallel conductive fibers that can transport electrons along the longitudinal axis of the filament. However, if the fibers would act as independent conductive pathways, the resulting electrical network would be highly vulnerable to disruption. Any incidental damage to a fiber would immediately annihilate the associated electron transport channel along the entire length of the filament. Hence, one would expect an evolutionary drive towards an electrical interconnectivity between fibers. In order to evaluate whether fibers are electrically interconnected, we performed a set of perturbation experiments in which all fibers were cut via abrasive removal of material within a narrow zone during sequential contact mode imaging with C-AFM (Figure 3; Figure S5, Supporting Information). In a first set of experiments, cuts were made in consecutive cells of the filament (Figure 3A–C). A subsequent C-AFM image, shown in Figure 3C, reveals the

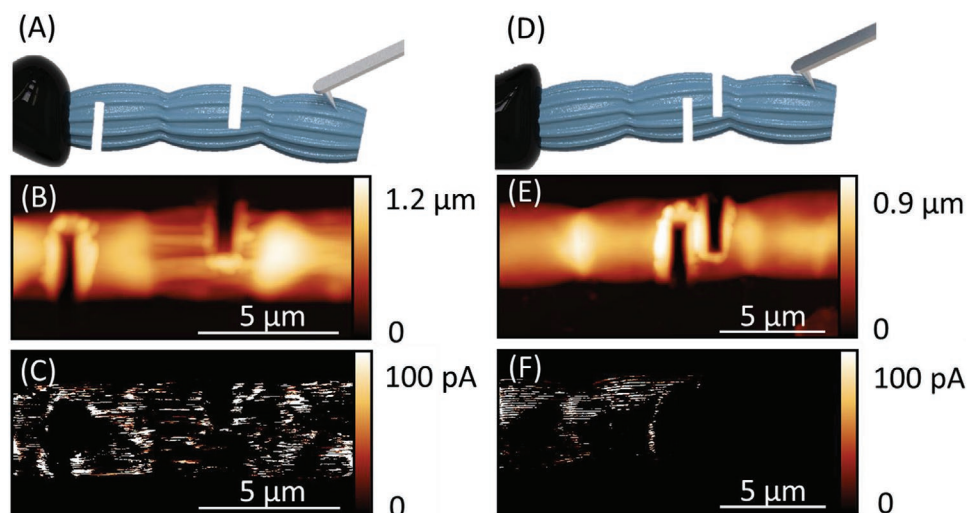


Figure 3. C-AFM imaging after deliberate filament cutting shows an electrical interconnection of fibers in the junctions between adjacent cells. A–C) When the two cuts are made in adjacent cells, currents can flow from the tip on the right side to the electrode on the left side, thus demonstrating there must be a connection between the fibers. D–F) When two opposite cuts are made within a single cell, the current vanishes on the right-hand side of the cuts, proving there is no longer a current path to the electrode located on the left-hand side. A,D) Scheme showing the electrical current path. B,E) Height images. C,F) Current images.

presence of conductivity all along the filament, and proves the existence of an interconnection between the fibers. However, remarkably, when the two cuts were made within the same cell (Figure 3D–F), conduction is no longer observed beyond the cuts. This indicates that the interconnection is located in between adjacent cells (see Figure S4 in the Supporting Information), and can be possibly attributed to the cartwheel structure mentioned before (Figure 1A). In a third experiment, we monitored the change in resistance after making a single trench within a filament cutting $\approx 50\%$ of the fibers (see Experimental Section in the Supporting Information). The filament resistance only increased by $29 \pm 28\%$ ($n = 17$; Table S2, Supporting Information), which is substantially less than the expected 100% increase (assuming that half of the fibers are cut and fibers have no electrical interconnection). This confirms that the electron transport through the fiber network remains highly efficient, even when significantly damaged.

Cable bacteria appear to have evolved an internal conductive network that is highly fail-safe. Our C-AFM measurements reveal that electrical currents are transported through a parallel network of conductive periplasmic fibers, which are redundantly interconnected at the cell junctions. This way, the conductive fiber network can be locally damaged while still allowing efficient electron transport along the axis of the filament, in agreement with recent experiments showing that LDET remains functional when intermediate cells cease to be metabolically active.^[27] While redundant electrical networks are present in natural microbial systems, such as electroactive biofilms,^[28,29] the conductive fiber network in cable bacteria shows a high degree of structural organization and forms an ordered network that is redundant within a single filamentous organism. Such an interconnected wiring configuration generates electrical robustness, which most likely provides an evolutionary advantage, as the organism as a whole can still perform LDET, and hence maintain its metabolic activity in the presence

of local defects to individual fibers. This demonstrates that nature has already invented highly ordered and fail-safe electrical networks long before the era of microelectronics.

Experimental Section

Cultivation and Specimen Preparation: Sediments containing cable bacterium filaments were collected from the creek bed of a salt marsh (51°26'21.6"N 4°10'08.3"E), which has previously been reported to grow cable bacteria.^[5] Cable bacterium filaments were enriched in laboratory sediment cores under oxygenated overlying water, isolated from the sediment and washed to remove sediment particles and attached bacteria, using the procedure as detailed in.^[22] This produces so-called "intact" filaments. "Fibers sheaths" were obtained from intact filaments using the sequential extraction procedure as described^[22,24]

For the C-AFM measurements, 1 cm × 1 cm diced Si wafers (Wafernet Inc., San Jose CA, USA) with a SiO₂ top layer (200-nm-thick) were mounted on stainless steel discs (15 mm diameter, Micro to Nano VOF, Haarlem, NL) using silver paste (Micro to Nano VOF, Haarlem, NL) as an adhesive. A single cable bacterium filament was placed on the substrate with custom-made glass hooks, either as an intact filament or a fiber sheath. An aqueous graphene dispersion (henceforth referred to as "carbon paste," EM-Tec C30 Micro to Nano, Haarlem, the Netherlands) was applied over one end of the cable bacterium filament to make an electrical connection to the steel disc (Figure 1). For the analysis on the fail-safeness, carbon paste was also applied to the free end of the filament (see Supporting Information for additional details). After fast, initial preparation of filament samples under ambient atmospheric conditions, they were stored for two minutes under vacuum inside the load lock of a glove box allowing the carbon paste to dry. Subsequently, samples were introduced into the glove box where the AFM is installed for C-AFM imaging.

Conductive Atomic Force Microscopy: C-AFM was performed using Bruker Multimode 8 AFM (Santa Clara, CA, USA) with a Nanoscope V controller. The AFM was housed within a custom-made glove box system under nitrogen atmosphere to prevent the decay of conductance of the bacterial filaments resulting from exposure to O₂.^[24] The glove box has a load lock to quickly purge the sample with N₂ before bringing it in.

Three types of electrical probes were used. Intact filaments still retain their outer membrane, which was impossible to remove with soft probes (Figure S1, Supporting Information). Hence, for intact filament imaging (Figures 1C,D and 3; Figures S2 and S5, Supporting Information), conductive diamond coated Tip – Noncontact/tapping mode – Long cantilever – Reflex coating (CDT-NCLR) probes supplied by NanoWorld AG (Neuchâtel, Switzerland) were used, containing a highly doped diamond coated tip (nominal spring constant 70 N m⁻¹). These probes have a macroscopic tip radius between 100 and 200 nm and are extremely wear resistant due to the diamond tip coating. Set points used were 2.5 μN for imaging, and 15 μN for making transversal filament cuts. For fiber sheath imaging (Figure 1E,F), Point Probe Plus Noncontact/TappingMode – Long Cantilever – PtIr5 Coating (PPP-NCLPt) was used, supplied by NanoWorld AG, which had a Pt-Ir5 coating on both sides of the cantilever (nominal spring constant 48 N m⁻¹). A set point of 2.2 μN was used for imaging with these probes. Due the smaller tip radius of PPP-NCLPt probes (<25 nm), an electrical image with a higher resolution was obtained. It is shown that the coating of the tip is of less importance compared to the stiffness of the cantilever, which is essential for electrical imaging of cable bacterium. However, where CDT-NCLR probes worked best for imaging intact filaments, PPP-NCLPt was most appropriate for fiber sheaths (see also Figure S3 in the Supporting Information). This could be attributed to the strength of outer membrane that requires abrasiveness of a coated diamond probe to remove it. Finally, SCM-PIT-V2 probes (Bruker, nominal spring constant 3 N m⁻¹) were also used, where the front side of the probe was coated with Pt-Ir (apex radius 25 nm). This much softer probe, for which a setpoint of 60 nN was used, did not significantly change the topography of bacteria and hence preserved the topography much better compared to stiffer cantilevers, thus enabling to correlate height and current in fiber sheaths (Figure 2). This probe only reveals small conductive areas of the surface at the junction, hence preserving the topography to a greater extent as compared to stiffer cantilevers.

The probe holder was electrically connected to a Peakforce Tunneling AFM (PF-TUNA) module, which in turn was connected to the Nanoscope V controller. Voltage bias was applied to the sample through the magnetic sample holder, and a standard sample bias of 0.5 V was applied. The microscope was used in ScanAsyst mode while localizing an area of interest to prevent unintentional damages due to lateral force applied by the probe while using contact AFM, and to obtain high resolution topography images, before switching to conductive contact mode.

Statistical Analysis: All AFM data were analyzed using the open source SPM analysis software Gwyddion.^[30] Sample size (*n*) and number of replicates (*m*) per sample are indicated for each experiment in the manuscript and listed in an overview in the Supporting Information. Quantitative data are presented as mean ± SD. Outliers are identified by a Chauvenet test.

Supporting Information

Supporting Information is available from the Wiley Online Library or from the author.

Acknowledgements

R.T.E. and R.B. contributed equally to this work. The authors thank the colleagues from X-LAB from Hasselt University and the Microbial Electricity team from University of Antwerp for discussions and feedback. Special thanks to H. T. S. Boschker, I. Cardinaletti, J. Drijkoningen, J. L. Hou, and S. Thijs for their insights and discussions. Thanks to K. Ceysens and T. Custers for the graphics. This research was financially supported by the Research Foundation Flanders (FWO project grant G031416N to FJRM and JM, FWO aspirant grant 1180517N to RB) and Dutch Research Council (NWO Vici grant 016.VICI.170.072

to FJRM). All measurements and data analysis were performed by R.T.E. and R.B. in equal contribution. J.M. and B.C. coordinated the study. Conceptualization and discussion were done by J.M., R.V., B.C., R.C., R.T.E., and R.B. Cable bacteria enrichment and fiber sheath extraction was performed by S.H.-M., R.B., and F.J.R.M. Funding was acquired by J.M., J.V., and F.J.R.M. Writing was done by R.B., R.T.E., J.M., B.C., and F.J.R.M., with contributions from all authors.

Conflict of Interest

The authors declare no conflict of interest.

Keywords

bioelectronics, cable bacteria, conductive AFM, electroactive bacteria

Received: January 6, 2020

Revised: April 16, 2020

Published online:

- [1] R. Schauer, N. Risgaard-Petersen, K. U. Kjeldsen, J. J. T. Bjerg, B. B. Jorgensen, A. Schramm, L. P. Nielsen, *ISME J.* **2014**, *8*, 1314.
- [2] F. J. R. Meysman, *Trends Microbiol.* **2018**, *26*, 411.
- [3] N. Risgaard-Petersen, M. Kristiansen, R. B. Frederiksen, A. L. Dittmer, J. T. Bjerg, D. Trojan, L. Schreiber, L. R. Damgaard, A. Schramm, L. P. Nielsen, *Appl. Environ. Microbiol.* **2015**, *81*, 6003.
- [4] H. Müller, J. Bosch, C. Griebler, L. R. Damgaard, L. P. Nielsen, T. Lueders, R. U. Meckenstock, *ISME J.* **2016**, *10*, 2010.
- [5] S. Y. Malkin, A. M. Rao, D. Seitaj, D. Vasquez-Cardenas, E.-M. Zetsche, S. Hidalgo-Martinez, H. T. Boschker, F. J. Meysman, *ISME J.* **2014**, *8*, 1843.
- [6] L. D. W. Burdorf, A. Tramper, D. Seitaj, L. Meire, S. Hidalgo-Martinez, E. M. Zetsche, H. T. S. Boschker, F. J. R. Meysman, *Biogeosciences* **2017**, *14*, 683.
- [7] D. Seitaj, R. Schauer, F. Sulu-Gambari, S. Hidalgo-Martinez, S. Y. Malkin, L. D. W. Burdorf, C. P. Slomp, F. J. R. Meysman, *Proc. Natl. Acad. Sci. USA* **2015**, *112*, 13278.
- [8] C. Pfeffer, S. Larsen, J. Song, M. Dong, F. Besenbacher, R. L. Meyer, K. U. Kjeldsen, L. Schreiber, Y. A. Gorby, M. Y. El-Naggar, K. M. Leung, A. Schramm, N. Risgaard-Petersen, L. P. Nielsen, *Nature* **2012**, *491*, 218.
- [9] L. P. Nielsen, N. Risgaard-Petersen, H. Fossing, P. B. Christensen, M. Sayama, *Nature* **2010**, *463*, 1071.
- [10] J. T. Bjerg, H. T. S. Boschker, S. Larsen, D. Berry, M. Schmid, D. Millo, P. Tataru, F. J. R. Meysman, M. Wagner, L. P. Nielsen, A. Schramm, *Proc. Natl. Acad. Sci. USA* **2018**, *115*, 5786.
- [11] R. Marcus, *J. Electroanal. Chem.* **1997**, *438*, 251.
- [12] C. C. Moser, J. M. Keske, K. Warncke, R. S. Farid, P. L. Dutton, *Nature* **1992**, *355*, 796.
- [13] C. C. Page, C. C. Moser, X. Chen, P. L. Dutton, *Nature* **1999**, *402*, 47.
- [14] H. B. Gray, J. R. Winkler, *Biochim. Biophys. Acta.– Bioenerg.* **2010**, *1797*, 1563.
- [15] G. Reguera, K. D. McCarthy, T. Mehta, J. S. Nicoll, M. T. Tuominen, D. R. Lovley, *Nature* **2005**, *435*, 1098.
- [16] S. Xu, A. Barrozo, L. M. Tender, A. I. Krylov, M. Y. El-Naggar, *J. Am. Chem. Soc.* **2018**, *140*, 10085.
- [17] D. J. Walker, R. Y. Adhikari, D. E. Holmes, J. E. Ward, T. L. Woodard, K. P. Nevin, D. R. Lovley, *ISME J.* **2018**, *12*, 48.
- [18] D. J. F. Walker, E. Martz, D. E. Holmes, Z. Zhou, S. S. Nonnenmann, D. R. Lovley, *mBio* **2019**, *10*, <https://doi.org/10.1128/mBio.00579-19>.

- [19] D. J. F. Walker, K. P. Nevin, D. E. Holmes, A.-E. Rotaru, J. E. Ward, T. L. Woodard, J. Zhu, T. Ueki, S. S. Nonnenmann, M. J. McInerney, D. R. Lovley, *ISME J.* **2020**, *14*, 837.
- [20] K. U. Kjeldsen, L. Schreiber, C. A. Thorup, T. Boesen, J. T. Bjerg, T. Yang, M. S. Dueholm, S. Larsen, N. Risgaard-Petersen, M. Nierychlo, M. Schmid, A. Bøggild, J. van de Vossenberg, J. S. Geelhoed, F. J. R. Meysman, M. Wagner, P. H. Nielsen, L. P. Nielsen, A. Schramm, *Proc. Natl. Acad. Sci. USA* **2019**, *116*, 19116.
- [21] L. D. W. Burdorf, S. Y. Malkin, J. T. Bjerg, P. van Rijswijk, F. Criens, A. Tramper, F. J. R. Meysman, *Limnol. Oceanogr.* **2018**, *63*, 1799.
- [22] R. Cornelissen, A. Bøggild, R. Thiruvallur Eachambadi, R. I. Koning, A. Kremer, S. Hidalgo-Martinez, E.-M. Zetsche, L. R. Damgaard, R. Bonn , J. Drijkoningen, J. S. Geelhoed, T. Boesen, H. T. S. Boschker, R. Valcke, L. P. Nielsen, J. D'Haen, J. V. Manca, F. J. R. Meysman, *Front. Microbiol.* **2018**, *9*, 3044.
- [23] Z. Jiang, S. Zhang, L. H. Klausen, J. Song, Q. Li, Z. Wang, B. T. Stokke, Y. Huang, F. Besenbacher, L. P. Nielsen, M. Dong, *Proc. Natl. Acad. Sci. USA* **2018**, *115*, 201807562.
- [24] F. J. R. Meysman, R. Cornelissen, S. Trashin, R. Bonn , S. Hidalgo-Martinez, J. van der Veen, C. J. Blom, C. Karman, J. L. Hou, R. T. Eachambadi, J. S. Geelhoed, K. De Wael, H. J. E. Beaumont, B. Cleuren, R. Valcke, H. S. J. van der Zant, H. T. S. Boschker, J. V. Manca, *Nat. Commun.* **2019**, *10*, <https://doi.org/10.1038/s41467-019-12115-7>.
- [25] R. Y. Adhikari, N. S. Malvankar, M. T. Tuominen, D. R. Lovley, *RSC Adv.* **2016**, *6*, 8354.
- [26] S. Sure, A. A. J. Torriero, A. Gaur, L. H. Li, Y. Chen, C. Tripathi, A. Adholeya, M. L. Ackland, M. Kochar, *Antonie Van Leeuwenhoek* **2016**, *109*, 475.
- [27] N. M. J. Geerlings, C. Karman, S. Trashin, K. S. As, M. V. M. Kienhuis, *Proc. Natl. Acad. Sci. USA* **2020**, *117*, 5478.
- [28] M. V. Ord nez, G. D. Schrott, D. A. Massazza, J. P. Busalmen, *Energy Environ. Sci.* **2016**, *9*, 2677.
- [29] N. S. Malvankar, M. Vargas, K. P. Nevin, A. E. Franks, C. Leang, B. C. Kim, K. Inoue, T. Mester, S. F. Covalla, J. P. Johnson, V. M. Rotello, M. T. Tuominen, D. R. Lovley, *Nat. Nanotechnol.* **2011**, *6*, 573.
- [30] D. Ne as, P. Klapetek, *Open Phys.* **2012**, *10*, 181.